



Search for the Associated Production of Chargino and Neutralino in Final States with three Leptons with the DØ detector

The DØ Collaboration
URL: <http://www-d0.fnal.gov>
(Dated: March 9, 2007)

A search has been performed for the trilepton decay signature from the associated production of the lightest chargino and the next-to-lightest neutralino in leptonic channels of two muons plus a third lepton; and one muon and one electron plus a third lepton in the context of minimal Supersymmetry. The search uses data taken with the DØ detector at the Fermilab Tevatron $p\bar{p}$ collider at a center-of-mass energy of 1.96 TeV corresponding to an integrated luminosity of around 1 fb^{-1} . No candidates have been found in the $e\mu\ell$ channel with an expected background of $0.94^{+0.40}_{-0.13}$ events, while two candidates were found in the $\mu\mu\ell$ channel consistent with the background expectation of $0.30^{+0.73}_{-0.03}$ events. In combination with the results of two previously approved DØ trilepton analyses, new stringent limits on the associated production of charginos and neutralinos have been set.

Preliminary Results for Winter 2007 Conferences

I. INTRODUCTION

Supersymmetry (SUSY [1]) postulates a symmetry between bosonic and fermionic degrees of freedom and predicts the existence of a supersymmetric partner for each standard model particle. The present note describes the search for the associated production of the charged and neutral partners of the SM bosons (charginos and neutralinos) in final states with either one electron, one muon, a third lepton and large missing transverse energy (\cancel{E}_T), called $e\mu\ell$ in the following; or two muons, a third lepton and large \cancel{E}_T , called $\mu\mu\ell$. The analyses are based on the Minimal Supersymmetric extension of the Standard Model (MSSM) with R-parity conservation [1]. More specifically, we use a minimal supergravity (mSUGRA) inspired model with chargino ($\tilde{\chi}_2^0$) and neutralino ($\tilde{\chi}_1^\pm$) masses following the relation $m_{\tilde{\chi}_1^\pm} \approx m_{\tilde{\chi}_2^0} \approx 2m_{\tilde{\chi}_1^0}$. The model predicts pair production of the lightest chargino along with the second-lightest neutralino with subsequent decays into fermions and the LSP (the lightest supersymmetric particle, $\tilde{\chi}_1^0$) [2].

The points in mSUGRA parameter space considered here are characterized by slepton masses close to the chargino/neutralino masses, which lead to an enhanced leptonic branching fraction. The chargino/neutralino decay mode depends on the mass relation to the scalar partners of the charged leptons (sleptons). See Fig. 1 for an example of decay via off-shell gauge bosons and sleptons. For simplicity, the result is interpreted in a scenario without slepton mixing and degenerate \tilde{e}_R , $\tilde{\mu}_R$ and $\tilde{\tau}_R$ masses. Searches for supersymmetric particles have been performed in e^+e^- collisions at LEP [3] and in $p\bar{p}$ collisions at DØ [4], [5] and CDF [6]. No evidence for these particles has been found so far. LSP masses below 40 GeV are excluded in MSSM models with GUT relations by the LEP experiments. In mSUGRA, the LSP lower mass limit is found at 50–60 GeV [3]. For large slepton/sneutrino masses, chargino masses are excluded nearly up to the kinematic production threshold of 103 GeV at LEP [3] by direct searches. Higgs searches at LEP yield indirect sensitivity also for the mass region beyond the chargino production threshold.

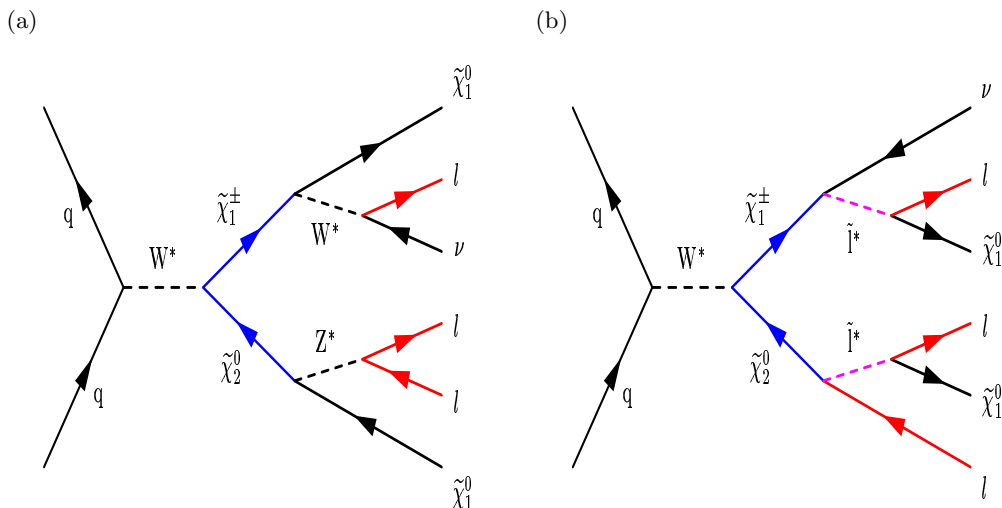


FIG. 1: Main production and decay modes for the signal points considered in the present analysis.

II. DATA AND MC SAMPLES

The analysis is based on data collected from April 2002 to February 2006 by the DØ detector at the Fermilab Tevatron $p\bar{p}$ collider at a center-of-mass energy of 1.96 TeV and corresponds to an integrated luminosity of 1.1 fb^{-1} . The luminosity is determined by normalizing MC to data around the Z peak at preselection level, using the NNLO cross section 241.6 pb , [7], [8]. All simulated signal and standard model processes are generated using PYTHIA 6.319 [9] and processed through the full detector simulation. Signal parameter combinations have been generated for $\tan\beta = 3$ and chargino masses in the range of 98–150 GeV using the parameters corresponding to the Les Houches Accords, (LHA) [10]. See Table I. Three reference points were chosen with low, medium and high $\tilde{\chi}^\pm$ mass within this mass range. The symbols in Table I are: The common fermion mass at GUT scale, $m_{1/2}$, the common scalar mass at GUT scale, m_0 , the ratio of vacuum expectation values of the two Higgs fields, $\tan\beta$, the trilinear coupling A_0 at GUT scale and the Higgs(ino) mass parameter, μ . The total cross section $\sigma \times \text{BF}(p\bar{p} \rightarrow \tilde{\chi}_1^\pm \tilde{\chi}_2^0 \rightarrow 3\ell)$ varies between 0.5 and 0.1 pb. A detailed description of the generated reference points is given in Table I.

Major background sources are $Z/\gamma \rightarrow \ell\ell$, $W + \gamma \rightarrow \ell\nu + \gamma$, and $WW \rightarrow \ell\nu\nu$. Multijet background from QCD production is determined directly from data in both analyses. Samples dominated by multijet background have been defined that are identical to the search samples except reversed lepton identification requirements. These samples will be called “fake” samples below. For the $e\mu\ell$ analysis, the electron ID variables and the muon isolation variables have been inverted in order to define a region in phase space where QCD is dominant. A sample of like-sign leptons is used to normalize the fake sample. The like-sign sample is dominated by QCD events at preselection level, but cannot be used in advanced stages of the analysis, since the signal is partly like sign. In the $\mu\mu\ell$ analysis, both muons are required to be non-isolated in the fake sample. Again, the sub-sample of the dataset consisting of like-sign events is used for normalization of the fake sample. The fake sample is also reweighted as a function of p_T in order to take into account the differences in the kinematics between the two samples.

name	$\tilde{\chi}^\pm$ -mass (GeV)	$\tilde{\chi}_2^0$ -mass (GeV)	$\tilde{\chi}_1^0$ mass (GeV)	m_0 (GeV)	$m_{1/2}$ (GeV)	$m_{\tilde{t}_R}$ (GeV)	$\sigma \times BR[pb]$
LHA.244.324	150	152	82	121	221	153	0.058
LHA.131.232	125	127	69	98	192	129	0.14
LHA. 87.194	115	118	63	88	182	119	0.22

TABLE I: SUSY parameters for three reference signal points. All points have $\tan\beta = 3$, $A_0 = 0$, $\mu > 0$.

III. EVENT SELECTION $e\mu\ell$

For the $e\mu\ell$ analysis, the selection criteria are discussed in detail below and are summarized in Table II. The events selected must have at least one electron with $p_T > 12$ GeV and one muon with $p_T > 8$ GeV. The electron-muon invariant mass must also exceed 15 GeV. Both leptons should stem from the same vertex ($\Delta z(e, \mu) < 1.5$ cm) and from the primary vertex, PV, ($\Delta z(\text{lepton}, \text{PV}) < 2.0$ cm). All leptons in the event are required to be well separated in space $\Delta R = \sqrt{\Delta\eta^2 + \Delta\phi^2} > 0.4$. To remove possible contributions from WZ decays, events are vetoed if two electrons or two muons are found in the event and their invariant mass is larger than 70 GeV. These cuts are referred as “Cut 1” (preselection). The largest contribution to the background at this stage is multi-jet events from QCD production, Z/γ^* decays and from $W + jet/\gamma$ events.

Events from QCD and Z/γ^* contributions can be effectively rejected with a cut on the missing transverse energy \cancel{E}_T and on the minimum transverse mass $M_{min}^T(\ell, \cancel{E}_T)$ (“Cut 2”). Fig. 2a shows the \cancel{E}_T distribution at preselection level and Fig. 2b shows the $M_{min}^T(\ell, \cancel{E}_T)$ distribution at preselection level. QCD events are characterized by small values of \cancel{E}_T , while the two LSPs and the neutrinos in the signal topology lead to a considerable amount of \cancel{E}_T . Therefore, events with $\cancel{E}_T < 10$ GeV are discarded.

Larger values of \cancel{E}_T can also be mimicked due to poorly measured lepton energy and thus small angles between \cancel{E}_T and one of the leptons. This leads to small values of the transverse mass of the lepton with the missing transverse energy, whereas the signal is characterised by larger transverse masses. The cut on the minimal transverse mass $M_{min}^T(\ell, \cancel{E}_T)$ is applied at $M_{min}^T(\ell, \cancel{E}_T) > 20$ GeV. An upper cut of $M_{min}^T(\ell, \cancel{E}_T) < 90$ GeV removes a fraction of WW events without decreasing the signal efficiency.

In addition, events are rejected if they contain jets with transverse energies above 15 GeV and have a small missing ET significance, $\text{Sig}(\cancel{E}_T)$, which is defined by normalizing the \cancel{E}_T to $\sigma_{E_T^j \parallel \cancel{E}_T}$, a measure of the jet energy resolution projected onto the \cancel{E}_T direction, (“Cut 3”):

$$\text{Sig}(\cancel{E}_T) = \frac{\cancel{E}_T}{\sqrt{\sum_{\text{jets}} \sigma_{E_T^j \parallel \cancel{E}_T}^2}}.$$

At this selection stage, the dominant backgrounds are $W + jet$ events and pair production of W bosons. A cut on the electron-muon invariant mass $M_{e\mu}$ is expected to reduce both backgrounds, since most of these events have large invariant mass. The $M_{e\mu}$ invariant mass is required to be less than 100 GeV (“Cut 4”). See Fig. 2c for the $M_{e\mu}$ invariant mass distribution at preselection level. $t\bar{t}$ events are further rejected by requiring $H_T < 50$ GeV (“Cut 5”), the scalar sum of the p_T of the jets in the event. Fig. 2d shows the H_T distribution after cut 4.

The next step in the selection is the identification of a third track. The selection of the track is designed to be efficient for all three charged leptons. The track has to be well separated from electron and muon ($\Delta R(e/\mu, \text{track}) = \sqrt{\Delta\eta^2 + \Delta\phi^2} > 0.4$), but come from the same vertex ($\Delta z(\text{track}, e/\mu) < 1.0$ cm). Two isolation criteria are applied. In order to reduce events with tracks from charged hadrons within a jet, tracker isolation is applied by requiring that

Selection criterion	Value
Cut 1 Preselection	Trigger, ID, no charge requirement $p_T^e > 12$ GeV and $p_T^\mu > 8$ GeV, $m_{ll} > 15$ GeV $\Delta z(e, \mu) < 1.5$ cm, $\Delta z(\ell, \text{PV}) < 2.0$ cm, $\Delta R(e, \mu) > 0.4$ remove events with $2e$ or 2μ , if M_{ee} or $M_{\mu\mu} > 70$ GeV
Cut 2 \cancel{E}_T	$\cancel{E}_T > 10$ GeV
$M_{min}^T(\ell, \cancel{E}_T)$	$20 \text{ GeV} < M_{min}^T(\ell, \cancel{E}_T) < 90 \text{ GeV}$
Cut 3 Sig(\cancel{E}_T)	Sig(\cancel{E}_T) > 8 (for $N_{Jet} > 0$)
Cut 4 Invariant mass $M_{ll'}$	$M_{e\mu} < 100$ GeV
Cut 5 H_T (scalar sum of p_T^{Jet})	$H_T < 50$ GeV
Cut 6 3^{rd} isolation track	$p_T(track) > 5.0$ GeV, tracker isolation $\Sigma p_T < 1$ GeV calorimeter isolation $E_{iso} < 3.0$ GeV and $E_{iso}/\text{GeV} < 0.6 * \sqrt{p_T(track)/\text{GeV}}$
Cut 7 $M_T(3^{rd} track, \cancel{E}_T)$	$M_T(3^{rd} track, \cancel{E}_T) > 8$ GeV
Cut 8 Anti WZ/γ^*	Remove events if $M(e, track) < 5$ GeV, $M(e, track) > 70$ GeV Remove events if $M(\mu, track) < 5$ GeV, $M(\mu, track) > 70$ GeV $p_T^{3^{rd} track} > 7$ GeV, if $60 \text{ GeV} < M_{max}^T(\ell, \cancel{E}_T) < 90 \text{ GeV}$

TABLE II: Summary of the selection criteria for $e\mu\ell$ final state.

the scalar p_T sum of all tracks in $0.1 < \Delta R < 0.4$ around the third track is $\Sigma p_T < 1$ GeV. Further reduction of number of tracks from QCD jets is achieved by cutting on the calorimeter energy deposition in a cone around the third track. The scalar sum of the transverse energy in a hollow cone $0.2 < \Delta R < 0.4$ around the track is required to be less than 3 GeV and $\frac{\Sigma E_T}{\text{GeV}} < 0.60 \sqrt{\frac{p_T^{\ell 3}}{\text{GeV}}}$ where $p_T^{\ell 3}$ denotes the p_T of the isolated track and ΣE_T is the scalar sum of the transverse energy in the electromagnetic and the fine hadronic cells.

After requiring an isolated track, the main backgrounds are $W^\pm \rightarrow \ell^\pm \nu$ and $Z/\gamma^* \rightarrow \mu\mu$, where in the second case the third track is coming from a non-reconstructed muon. These events passed the cuts dealing with \cancel{E}_T because the muon was not reconstructed and consequently \cancel{E}_T is overestimated by the amount of the transverse momentum of the muon and \cancel{E}_T points into the direction of muon. A significant fraction of this $Z/\gamma^* \rightarrow \mu\mu$ background can be suppressed by the cut on the transverse mass $M_T(3^{rd} track, \cancel{E}_T)$ of the third track and missing transverse energy: $M_T(3^{rd} track, \cancel{E}_T) > 8$ GeV (“Cut 7”). See Fig. 3a for the $M_T(3^{rd} track, \cancel{E}_T)$ distribution after cut 6 and Fig. 3b for the $\Delta\phi$ distribution between the third track and \cancel{E}_T .

At the last stage of the selection, the background from WZ remains the largest one. Therefore, a cut on the invariant mass of the electron and third track $M(e, track) < 70$ GeV or on the invariant mass of the muon and third track $M(\mu, track) < 70$ GeV is used to remove WZ contamination in events where one of the leptons from Z is reconstructed as a third track. Finally, the $W + jet$ and WW backgrounds are further suppressed by raising the p_T threshold of the third track to 7 GeV, if the transverse mass of the leading lepton and \cancel{E}_T is between 60 GeV and 90 GeV, making use of the fact that an additional track in W events has low- p_T (“Cut 8”). See Fig. 3c for the $M(\mu, track)$ distribution after cut 7.

IV. EVENT SELECTION $\mu\mu\ell$

The $\mu\mu\ell$ selection criteria are summarized in Table III. The selection requires two isolated muons with $p_T > 12$ and 8 GeV. See Fig. 4a and b for the p_T distributions of the leading μ and trailing μ at preselection level. Both muons have to stem from the primary vertex. The muons have to be isolated both in the tracker and in the calorimeter. The tracker isolation is defined as the sum of p_T of tracks found within a cone of $\Delta R < 0.5$ around the muon candidate

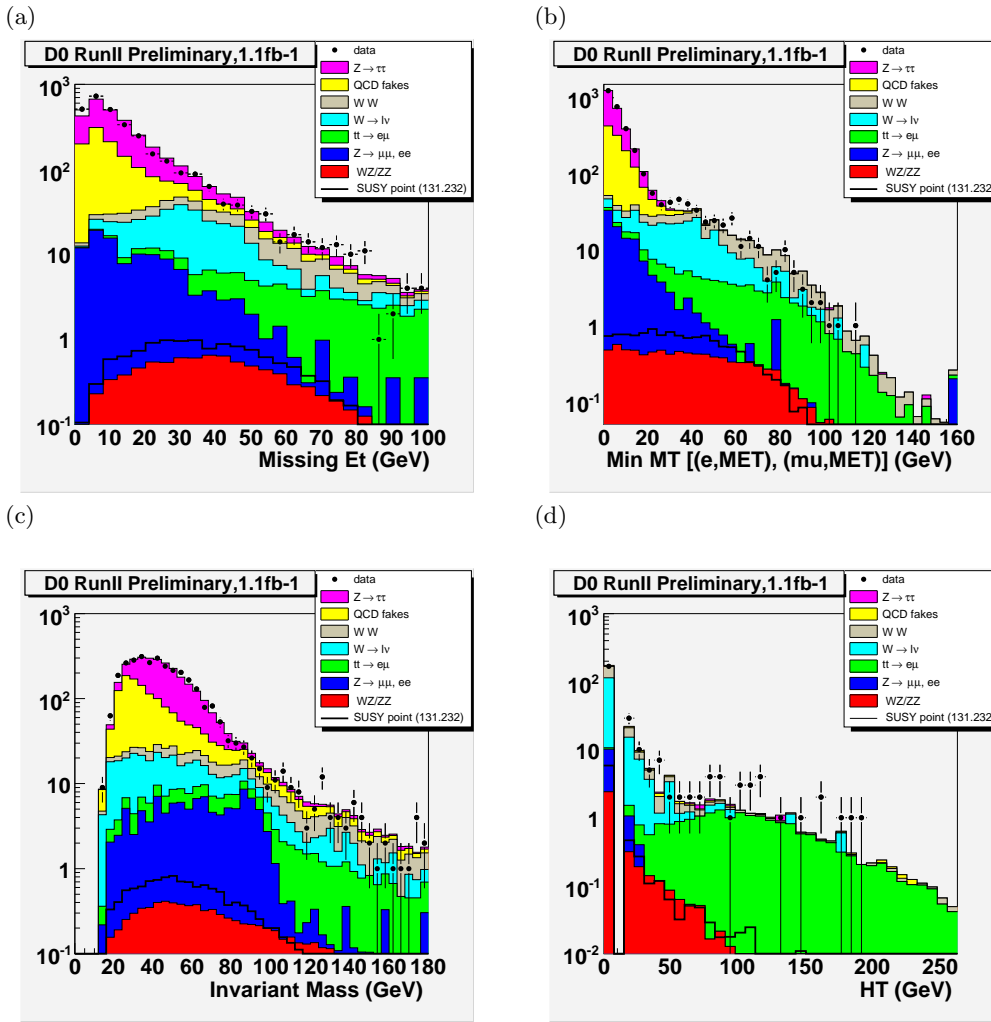


FIG. 2: $(e\mu\ell)$ Distribution of (a) the missing transverse energy, \cancel{E}_T at preselection level (b) M_T at preselection level, (c) invariant $e\mu$ mass at preselection level and (d) H_T after Cut 4, for data (points with error bars), background simulation (histograms, complemented with the QCD expectation) and signal expectation for point LHA.131.232 (empty histogram).

track. The calorimeter isolation is the sum of energy of cells within a hollow cone of $0.1 < \Delta R < 0.5$ around the position of the muon track in the calorimeter.

The leading muon must be isolated with $E_{\text{iso}} < 4$ GeV in the tracker and the calorimeter. The trailing muon must fulfill $E_{\text{iso}} < 1.5$ GeV. Many background processes have one isolated muon in the final state, whereas the second reconstructed muon lies within a jet. The tight requirement on the trailing muon reduces this background, especially the $W \rightarrow \mu\nu$ background.

The invariant mass of the muon pair must be $24 < M_{\mu\mu} < 60$ GeV. The criteria is chosen to reject $\Upsilon(nS)$ and Drell-Yan background on the lower edge and $Z \rightarrow \mu\mu$ background on the upper edge of the selected mass region. See Fig. 4c for the invariant mass distribution at preselection level.

The requirement $\Delta\phi(\mu_1, \mu_2) < 2.9$ rejects mainly background from Z decays and QCD background which both peak at $\Delta\phi = \pi$ whereas the signal is almost uniformly distributed in $\Delta\phi$. This cut also removes residual background from cosmics which are back-to-back. Fig. 4d shows the $\Delta\phi(\mu_1, \mu_2)$ distribution at preselection level.

As discussed in Section III, the trilepton signal to background ratio can be enhanced by requiring well-measured \cancel{E}_T using the following cuts on \cancel{E}_T , $\text{Sig}(\cancel{E}_T)$ and $M_T(\mu, \cancel{E}_T)$: $\cancel{E}_T > 20$ GeV, $\text{Sig}(\cancel{E}_T) > 8$, $M_T > 20$ GeV. See Fig. 5a for the \cancel{E}_T distribution at preselection level and Fig. 5b for the distribution of $\text{Sig}(\cancel{E}_T)$ at preselection level. The transverse momentum of the third track must be $p_T > 4$ GeV. Both isolation in the tracker and in the calorimeter are required. See Fig. 5c of the p_T distribution of the third track. For the third lepton a transverse mass $M_T(\text{track}, \cancel{E}_T) > 8$ GeV is required. This requirement removes a large fraction of the remaining $Z \rightarrow \mu\mu$ background. A fraction of the remaining WZ background can be removed by requiring that the invariant mass of the leading muon and the third track is below the Z mass: $M_{\mu_1\ell_3} < 80$ GeV.

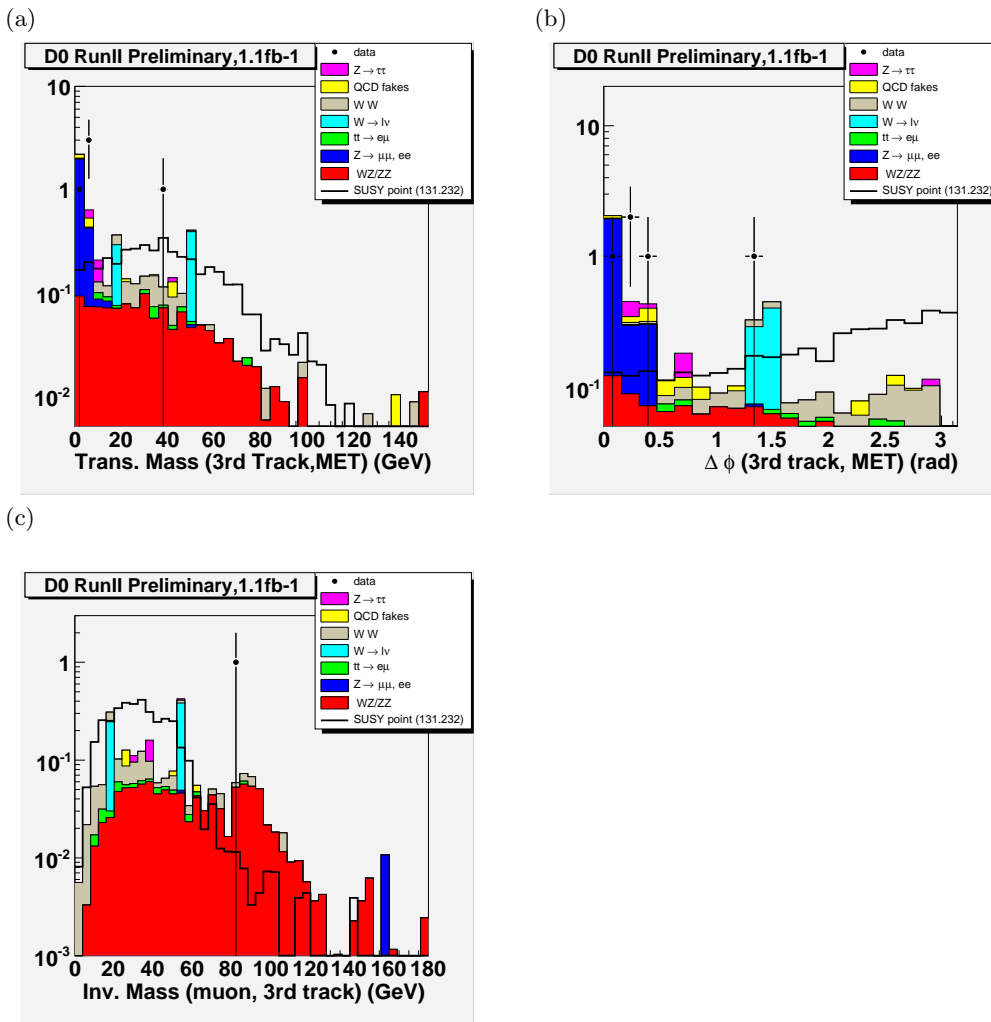


FIG. 3: ($e\mu\ell$)Distribution of (a) M_T between the third track and \cancel{E}_T after cut 6, (b) $\Delta\phi$ between \cancel{E}_T and third track after cut 6, (c) invariant mass between muon and third track after cut 7, for data (points with error bars), background simulation (histograms, complemented with the QCD expectation) and signal expectation for point LHA.131.232 (empty histogram).

In chargino and neutralino decays the p_T of the event is balanced between the chargino on one side and the neutralino on the other side. The ratio of the vector sum of the momenta of muons and \cancel{E}_T and the p_T of the third track is defined as p_T balance. For signal events this variable peaks around 1. Part of the WZ background has a p_T balance close to 0. QCD and background from Z decays have a large fraction of events with high values of the the p_T ratio. A selection of events with $0.3 < (p_T(\mu_1) + p_T(\mu_2) + \cancel{E}_T)/p_T(track) < 3$ is made.

For the remaining background the product of $\cancel{E}_T \times p_T(track)$ has low values. A cut on this variable is made: $\cancel{E}_T \times p_T(track) > 150 \text{ GeV}^2$, and the choice of 150 GeV^2 cuts away a relatively larger fraction of the remaining background than signal. (See Fig. 5d).

V. SYSTEMATIC UNCERTAINTIES

The estimates for expected numbers of background and signal events depend on numerous measurements that each introduce a systematic uncertainty: lepton identification, trigger efficiencies and reconstruction efficiencies (4%), jet energy scale calibration in signal ($< 1\%$) and background events (1%), lepton and track momentum calibration (1%), PDF uncertainties ($< 4\%$), and modeling of multijet background (30%). The systematic error on the luminosity is mainly a combination of the PDF uncertainty (4%), uncertainty for the NNLO Z cross section (4%) and data/MC normalization factor (2%). For the estimate of the background remaining after all cuts, the systematic uncertainties are small compared to the statistical uncertainty due to limited Monte Carlo statistics. See Table IV for the different sources of systematic uncertainties in the $e\mu\ell$ channel and Table V for the sources in the $\mu\mu\ell$ channel.

Selection criteria	Value
Cut 1 Preselection	Trigger, ID, $p_T^l > 12$ GeV and $p_T^{l'} > 8$ GeV calorimeter isolation < 4 (1.5) GeV, tracker isolation < 4 (1.5) GeV for the leading (trailing) muon both muons must come from the primary vertex
Cut 2 Mass:	$24 \text{ GeV} < M(\mu_1, \mu_2) < 60 \text{ GeV}$
Cut 3 $\Delta\phi$:	$\Delta\phi(\mu_1, \mu_2) < 2.9$
Cut 4 \cancel{E}_T	Missing Transverse Energy $\cancel{E}_T > 20$ GeV
Cut 5 Sig(\cancel{E}_T)	Sig(\cancel{E}_T): Sig(\cancel{E}_T) > 8 or 0 jets
Cut 6 Transverse Mass $\mu_{1,2}$	$M_T(\mu, \cancel{E}_T) > 20$ GeV for both muons
Cut 7 $p_T\ell_3$ (tr)	$p_T(\ell_3) > 4.0$ GeV, track isolation $\Sigma p_T < 1$ GeV
Cut 8 $p_T\ell_3$ (calo)	$p_T(\ell_3) > 4.0$ GeV, calo isolation $E_T < (3\text{GeV and } 0.60\sqrt{(p_T(\text{track}))/\text{GeV}})$
Cut 9 Transverse Mass ℓ_3	$M_T(\ell_3, \cancel{E}_T) > 8$ GeV for both muons
Cut 10 Mass $\mu_1\ell_3$	$M(\mu_1, \ell_3) < 80$ GeV
Cut 11 p_T balance	$0.3 < (p_T(\mu) + \cancel{E}_T)/p_T(\ell_3) < 3$
Cut 12 p_T product	$\cancel{E}_T * p_T(\ell_3) > 150 \text{ GeV}^2$

TABLE III: List of the cuts used for the $\mu\mu\ell$ final state.

Source	Background	Signal
QCD scale factor	3 %	-
Electron ID	2 %	$< 2\%$
Muon ID	2 %	$< 2\%$
Jet Energy Scale	15 %	5 %
WW scale/PDF	2 %	-
WZ scale/PDF	2 %	-
Quadratic sum	16 %	5 %
Luminosity (total)	6 %	6 %
(Z/γ^* scale,	4 %	-
Z/γ^* PDF	4 %	-
data/MC norm. factor)	2 %	-
Quadratic sum total	17 %	8 %

TABLE IV: ($e\mu\ell$) Systematic uncertainties on the number of events expected from Standard Model processes and from SUSY processes after the last selection cut (relative errors are quoted).

VI. RESULTS

Numbers of observed candidates and background events expected after application of the successive selections are listed in Table VI for $e\mu\ell$ and in Table VII for $\mu\mu\ell$. For the $e\mu\ell$ analysis, no candidates are observed. The background expectation is 0.94 ± 0.40 events, dominated by di-boson events. For $\mu\mu\ell$ the background expectation is 0.32 ± 1.34 and two events are selected in data. Also in the $\mu\mu\ell$ analysis di-boson events dominate the background composition at the final cut stage. The number of signal events is in the range of 0.89-3.03 events in the final selection for the three reference points mentioned in this note. Table VIII shows the number of signal events expected at different stages of the cutflow for three reference points for the $e\mu\ell$ analysis and in Table IX for the $\mu\mu\ell$ analysis.

Since no evidence for associated production of charginos and neutralinos is observed, an upper limit on the product of cross section and leptonic branching fraction $\sigma \times \text{BR}(3\ell)$ is extracted from this result. The result of these two

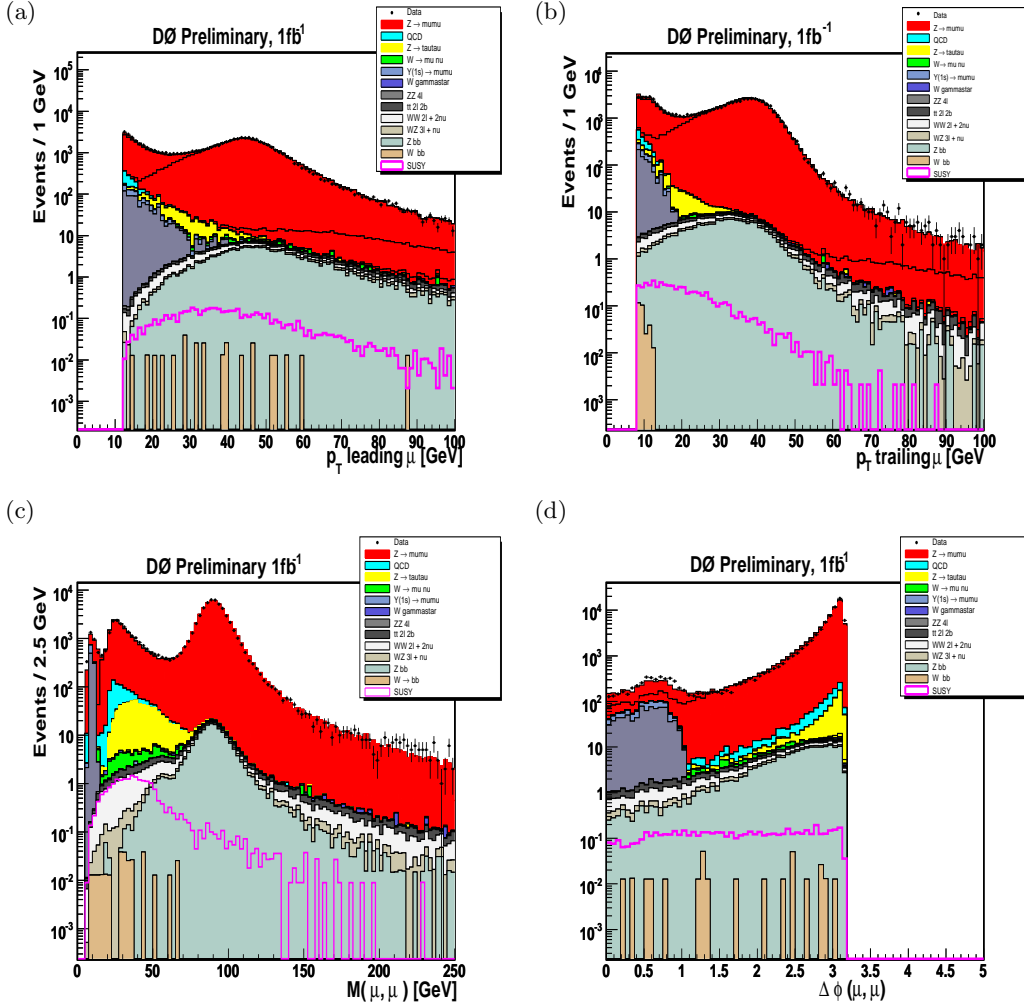


FIG. 4: $(\mu\mu\ell)$ Distribution of (a) p_T of leading μ at preselection level (b) p_T of trailing μ at preselection level, (c) di-muon invariant mass at preselection level, (d) $\Delta\phi(\mu, \mu)$ at preselection level, for data (points with error bars), background simulation (histograms, complemented with the QCD expectation) and signal expectation for point LHA.131.232 (open histogram).

analyses are combined with the results of the $e\ell\ell$ [11], and like-sign $\mu\mu$ [12], using the modified frequentist approach. The fraction of signal events that is selected by more than one selection is assigned to the selection with the largest signal-to-background ratio and removed from all others. Correlated errors are taken into account. The expected and observed limits are shown in Fig. 6 as a function of $\tilde{\chi}_1^\pm$ mass. The result improves the upper limit of about 0.1 pb set by [11].

Assuming the mSUGRA-inspired mass relation $m_{\tilde{\chi}_1^\pm} \approx m_{\tilde{\chi}_2^0} \approx 2m_{\tilde{\chi}_1^0}$ as well as degenerate slepton masses $m_{\tilde{\ell}}$ (no slepton mixing), the limit on $\sigma \times \text{BR}(3\ell)$ is a function of $m_{\tilde{\chi}_1^\pm}$ and $m_{\tilde{\ell}}$ with a relatively small dependence of the other SUSY parameters. This result can therefore be interpreted in more general SUSY scenarios as long as the above mass relations are satisfied and R -parity is conserved. The leptonic branching fraction of chargino and neutralino depends on the relative contribution from the slepton- and W/Z -exchange graphs, which varies as a function of the slepton masses. W/Z exchange is dominant at large slepton masses, resulting in relatively small leptonic branching fractions (large m_0 scenario). The leptonic branching fraction for three-body decays is maximally enhanced for $m_{\tilde{\ell}} \gtrsim m_{\tilde{\chi}_2^0}$ (3ℓ -max scenario). In addition, the $\tilde{\chi}_1^\pm \tilde{\chi}_2^0$ production cross section depends on the squark masses due to the negative interference with the t-channel squark exchange. Relaxing scalar mass unification, the cross section is maximal in the limit of large squark masses (heavy-squarks scenario)

For the 3ℓ -max scenario, the updated tripleton analyses have improved the sensitivity in terms of the expected limit on the chargino mass from 117 GeV, [5], to 137 GeV. The new observed limit on the chargino mass is 141 GeV.

Decays into leptons can even be dominant if sleptons are light enough that two-body decays are possible. In the latter case, one of the leptons from the neutralino decay can have a very low transverse momentum if the mass

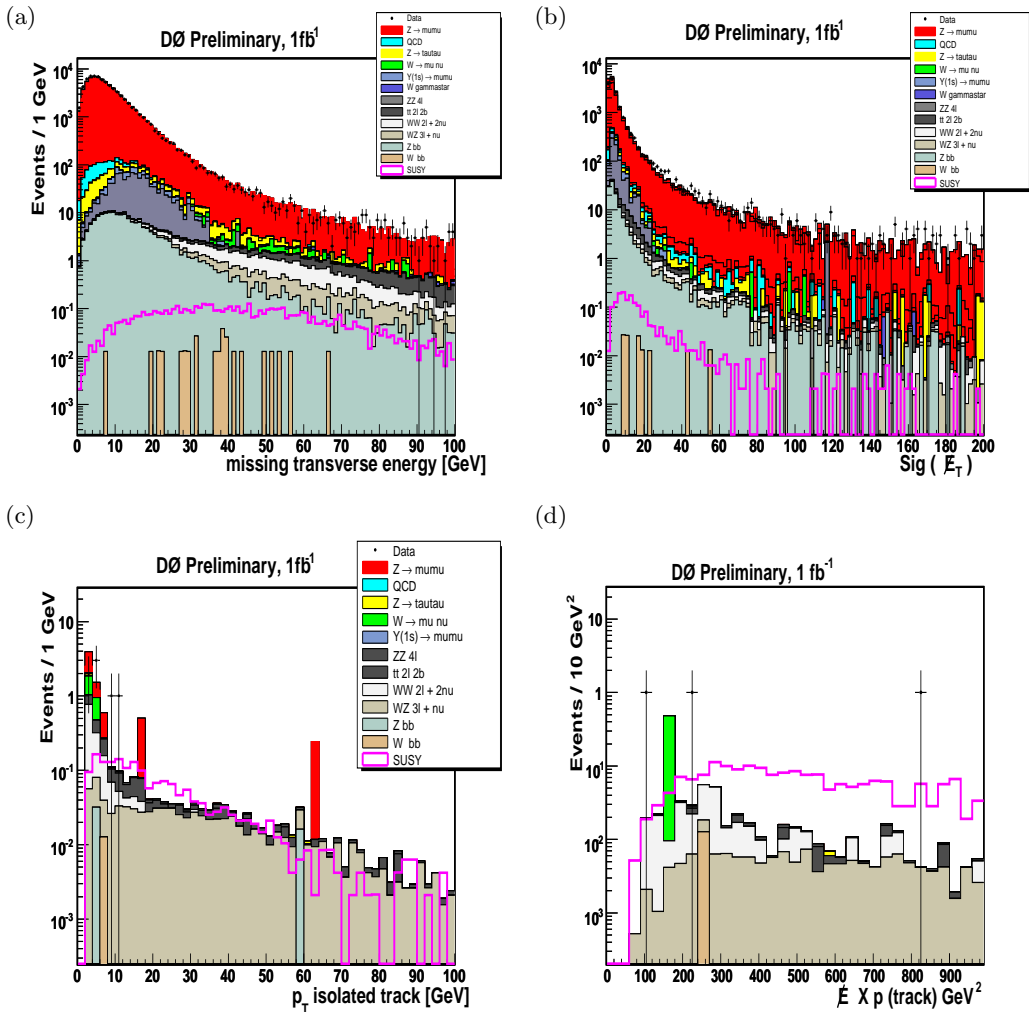


FIG. 5: $(\mu\mu\ell)$ Distribution of (a) \cancel{E}_T at preselection level, (b) $\text{Sig}(\cancel{E}_T)$ at preselection level, (c) $p_T^{\ell 3}$ of the third track before an isolated track is required in the event, (d) p_T product before the cut is applied, for data (points with error bars), background simulation (histograms, complemented with the QCD expectation) and signal expectation for point LHA.131.232 (open histogram).

difference between neutralino and sleptons is small. In this region, only the $\mu^\pm\mu^\pm$ selection remains efficient, leading to a slightly higher limit for $-6 \lesssim m_{\tilde{\ell}} - m_{\tilde{\chi}_2^0} \leq 0$. (see Fig. 7).

VII. CONCLUSIONS

A search has been performed for the trilepton decay signature from the associated production of the lightest chargino and the next-to-lightest neutralino in leptonic channels with one electron, one muon and a third lepton and two muons and a third lepton, using data corresponding to an integrated luminosity of 1.1fb^{-1} . No evidence for supersymmetry is observed and new upper limits on the product of cross section and leptonic branching fraction are set, which are more stringent than all existing limits for chargino masses beyond the LEP reach. Chargino mass limits beyond the reach of LEP chargino searches are derived for several SUSY reference scenarios with enhanced leptonic branching fractions.

Source	Background	Signal
Muon ID, trigger, reconstruction	4%	4%
QCD scale factor	13 %	-
Jet Energy Scale	< 1%	< 1%
WW scale/PDF	1 %	-
WZ scale/PDF	1 %	-
Track Momentum	1 %	1%
$Z \rightarrow \mu\mu$ at large M_T	17%	-
Quadratic sum	21.8 %	4.25 %
Luminosity (total)	6 %	6 %
(Z/γ^* scale)	4 %	-
Z/γ^* PDF	4 %	-
data/MC norm. factor)	2 %	-
Quadratic sum total	22.6 %	7.4 %

TABLE V: ($\mu\mu\ell$) Systematic uncertainties on the number of events expected from Standard Model processes and from SUSY processes after the last selection cut.

TABLE VI: Number of candidate events observed and background events expected at different stages of the $e\mu\ell$ selection. Uncertainties are statistical.

Cut	Data	Sum BG	$Z/\gamma^* \rightarrow \tau\tau$	$W \rightarrow \ell\nu$	fakes	WZ/ZZ	WW	$Z/\gamma^* \rightarrow ee, \mu\mu$
(1) PreSel	3105	3080 ± 34	1563 ± 10	221 ± 8	986 ± 31	8.8 ± 0.2	130 ± 1	103 ± 4
(2) \cancel{E}_T related	303	287 ± 7	4.1 ± 0.4	145 ± 7	6.7 ± 2.6	4.9 ± 0.1	89 ± 1	9.5 ± 1.0
(3) Isolated Track	5	5.1 ± 0.9	0.2 ± 0.08	0.55 ± 0.4	0.2 ± 0.1	1.1 ± 0.1	0.5 ± 0.1	2.2 ± 0.5
(4) Anti-diboson	0	$0.94^{+0.40}_{-0.13}$	0.09 ± 0.04	$0.0^{+0.4}_{-0.0}$	0.04 ± 0.04	0.43 ± 0.04	0.3 ± 0.05	$0.0^{+0.1}_{-0.0}$

Acknowledgments

2/6/07 We thank the staffs at Fermilab and collaborating institutions, and acknowledge support from the DOE and NSF (USA); CEA and CNRS/IN2P3 (France); FASI, Rosatom and RFBR (Russia); CAPES, CNPq, FAPERJ, FAPESP and FUNDUNESP (Brazil); DAE and DST (India); Colciencias (Colombia); CONACyT (Mexico); KRF and KOSEF (Korea); CONICET and UBACyT (Argentina); FOM (The Netherlands); PPARC (United Kingdom); MSMT (Czech Republic); CRC Program, CFI, NSERC and WestGrid Project (Canada); BMBF and DFG (Germany); SFI (Ireland); The Swedish Research Council (Sweden); Research Corporation; Alexander von Humboldt Foundation; and the Marie Curie Program.

-
- [1] H.P. Nilles, Phys. Rep. **110** (1984) 1;
H.E. Haber and G.L. Kane, Phys. Rep. **117** (1985) 75.
[2] W.Beenakker *et al.*, ‘The production of Charginos/Neutralinos and Stoptons at Hadron Colliders’, hep-ph/9906298.
[3] LEPSUSYWG, ALEPH, DELPHI, L3 and OPAL experiments,

TABLE VII: Number of candidate events observed and background events expected at different stages of the $\mu\mu\ell$ selection. Uncertainties are statistical.

Cut	Data	Sum BG	$Z/\gamma^* \rightarrow \mu\mu$	$W \rightarrow \mu\nu$	$Z/\gamma^* \rightarrow \tau\tau$	WW/ZZ	WZ	fakes
(1) PreSel	81927	80373 ± 130	78626 ± 130	45.6 ± 4.5	645 ± 9	60.1 ± 0.4	14.3 ± 0.07	754 ± 26
(2) Anti-Z	7486	8099 ± 53	7641 ± 53	27.5 ± 3.5	159 ± 5	19.3 ± 0.3	1.73 ± 0.03	233 ± 14
(3) \cancel{E}_T related	51	54 ± 4	31.4 ± 3.4	14.5 ± 2.6	0.54 ± 0.29	14.0 ± 0.2	1.20 ± 0.02	0.99 ± 0.99
(4) Isolated Track	4	$0.92^{+0.75}_{-0.04}$	1.3 ± 0.7	0 ± 0.5	0 ± 0.29	0.35 ± 0.03	0.54 ± 0.01	0.42 ± 0.42
(5) $\text{Tr} \times \cancel{E}_T$	2	$0.32^{+0.73}_{-0.03}$	$0.0^{+0.7}_{-0.0}$	$0.0^{+0.5}_{-0.0}$	$0.0^{+0.29}_{-0.0}$	0.15 ± 0.02	0.14 ± 0.007	< 0.42

TABLE VIII: Number of signal events expected at different stages of selection with statistical uncertainties for the $e\mu\ell$ final state. Uncertainties are statistical. For the final cut the signal efficiency in (%) is also presented. Efficiencies are normalized to the number of lepton events with all flavour combinations.

CUT	LHA.244.324	LHA.131.232	LHA.87.194
(1) Presel	6.8 ± 0.11	14.4 ± 0.24	22.1 ± 0.4
(2) \cancel{E}_T related	4.6 ± 0.09	9.2 ± 0.20	13.9 ± 0.34
(3) Isolated Track	2.2 ± 0.06	4.6 ± 0.14	6.5 ± 0.23
(4) Anti-diboson	0.95 ± 0.04	2.8 ± 0.11	4.03 ± 0.19
efficiency (3ℓ) (%)	2.6 ± 0.09	2.2 ± 0.07	2.0 ± 0.08

TABLE IX: Number of signal events expected at different stages of the $\mu\mu\ell$ selection. Uncertainties are statistical. Signal efficiency (in %) relative to all lepton flavours are also given.

Cut	LHA.244.324	LHA.131.232	LHA.87.194
(1) Presel	3.56 ± 0.07	12.1 ± 0.24	17.9 ± 0.41
(2) Anti-Z	2.11 ± 0.06	7.75 ± 0.20	11.4 ± 0.34
(3) \cancel{E}_T related	1.49 ± 0.05	4.94 ± 0.16	6.94 ± 0.27
(4) Isolated track	0.85 ± 0.04	2.89 ± 0.12	4.05 ± 0.21
(5) $\text{Tr} \times \cancel{E}_T$	0.51 ± 0.03	1.83 ± 0.10	2.53 ± 0.16
efficiency (3ℓ) [%]	1.62 ± 0.08	1.73 ± 0.08	1.49 ± 0.07

note LEPSUSYWG/01-07.1. (<http://lepsusy.web.cern.ch/lepsusy/Welcome.html>)

- [4] B. Abbott *et al.*, Phys. Rev. Lett. **80** (1998) 8.
 [5] V. Abazov *et al.*, (DØ Collaboration), ‘Search for supersymmetry via associated production of charginos and neutralinos in final states with three leptons’, Phys. Rev. Lett. **95** (2005) 8.
 [6] F. Abe *et al.*, (CDF Collaboration) ‘Search for Chargino-Neutralino Associated Production at the Fermilab Tevatron Collider’, Phys. Rev. Lett. **80**, 5275 (1998). F. Abe *et al.*, (CDF Collaboration), ‘Combined limit for the trilepton analyses Summer 2006’, CDF note 8653.
 [7] R. Hamberg, W.L. van Neerven, and T. Matsuura, Nucl. Phys. **B359**, 343 (1991). [Erratum-ibid. **B644**, 403 (2002)].
 [8] T. Nunnemann, DØ Note 4476.

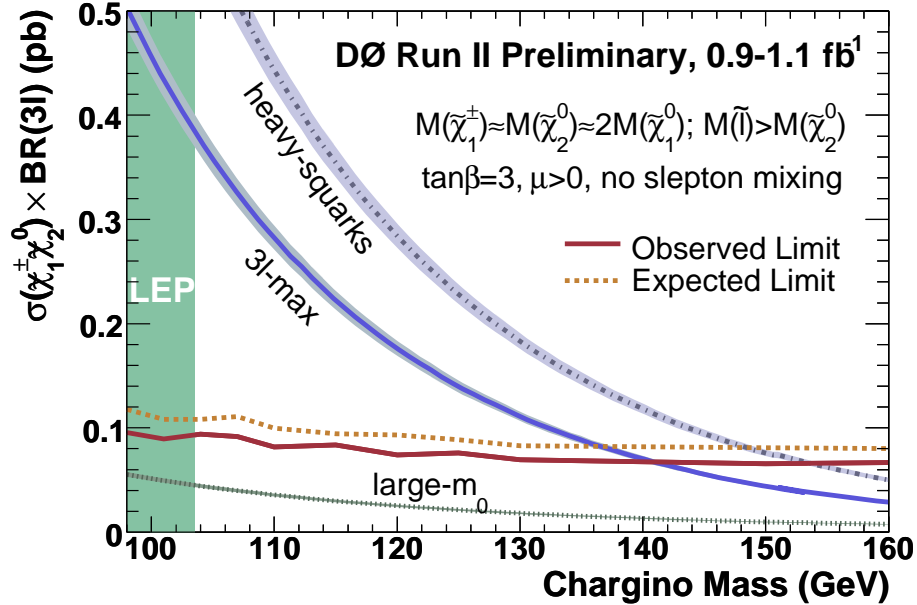


FIG. 6: Limit on $\sigma \times \text{BR}(3\ell)$ as a function of $\tilde{\chi}_1^\pm$ mass, in comparison with the expectation for several SUSY scenarios. The red line corresponds to observed mSUGRA limit. PDF and renormalization/factorization scale uncertainties are shown as shaded bands.

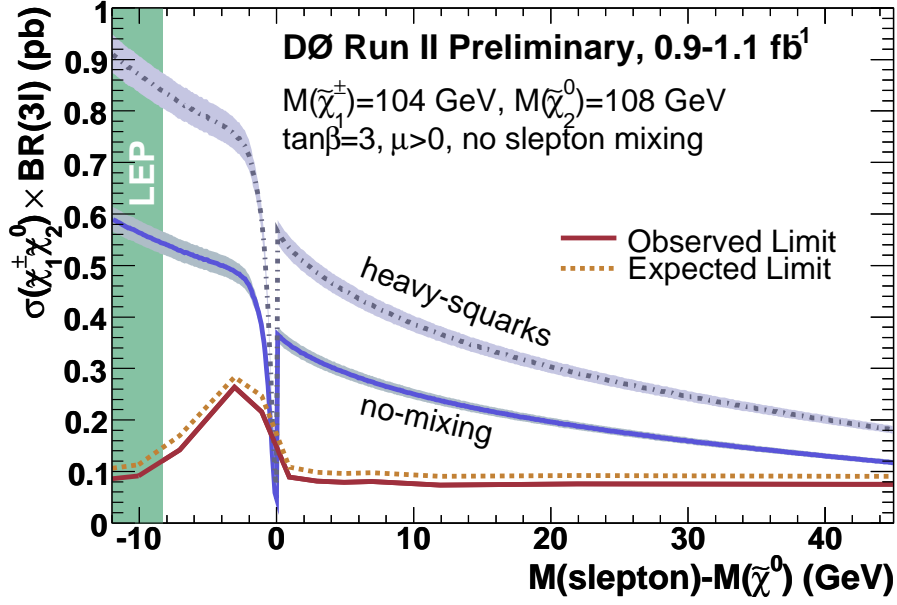


FIG. 7: Limit on $\sigma \times \text{BR}(3\ell)$ as a function of the mass difference between sleptons and $\tilde{\chi}_2^0$, in comparison with the expectation for the MSSM (no mixing) and the heavy-squarks scenario (see text). PDF and renormalization/factorization scale uncertainties are shown as shaded bands. $\text{BR}(3\ell)$ drops at $m_{\tilde{\ell}} \lesssim m_{\tilde{\chi}_2^0}$ as the phase space for two body decays into real sleptons is minimal.

- [9] T. Sjostrand, *Comp. Phys. Commun.* **82** (1994) 74, CERN-TH 7112/93 (1993).
- [10] P. Skands *et al.*, *JHEP* 07, 036 (2004).
- [11] V. Abazov *et al.*, (DØ Collaboration), ‘Search for the Associated Production of Charginos and Neutralinos in Final States with Two Electrons and an Additional Lepton’, DØ note 5127. (<http://www-d0.fnal.gov/Run2Physics/WWW/results/prelim/NP/N46/>)
- [12] V. Abazov *et al.*, (DØ Collaboration), ‘Search for the associated production of charginos and neutralinos in like sign dimuon channel’, DØ note 5126. (<http://www-d0.fnal.gov/Run2Physics/WWW/results/prelim/NP/N45/>)